
Article:
Ali, S.G., Ali, R., Bin, S. et al. (2022) Experimental protocol designed to employ Nd:YAG laser surgery for anterior chamber glaucoma detection via UBM. IET Image Processing, 16 (8). pp. 2171-2179. ISSN: 1751-9659

https://doi.org/10.1049/ipr2.12481

Received: 14 October 2021 | Accepted: 14 February 2022

DOI: 10.1049/ipr2.12481

IET Image Processing

The Institution of Engineering and Technology WILEY

ORIGINAL RESEARCH PAPER

Experimental protocol designed to employ Nd:YAG laser surgery for anterior chamber glaucoma detection via UBM

Saba Ghazanfar Ali[1] | **Riaz Ali**[2] | **Bin Sheng**[1] | **Yan Chen**[3] | **Huating Li**[3] | **Po Yang**[4] | **Ping Li**[5] | **Younhyun Jung**[6] | **Fang Zhu**[7,8] | **Ping Lu**[7,8] | **Jinman Kim**[9]

[1]Department of Computer Science and Engineering, Shanghai Jiao Tong University, Shanghai, China

[2]Department of Computer Science, Sukkur IBA University, Sukkur, Sindh, Pakistan

[3]Shanghai Jiao Tong University Affiliated Sixth People's Hospital, Shanghai, China

[4]Department of Computer Science, The University of Sheffield, Sheffield, U.K.

[5]Department of Computing, The Hong Kong Polytechnic University, Kowloon, Hong Kong

[6]Department of Software, Gachon University, Seongnam 13120, South Korea

[7]ZTE Corporation, Shenzhen, China

[8]State Key Laboratory of Mobile Network and Mobile Multimedia Technology, Shenzhen, China

[9]School of Computer Science, The University of Sydney, Sydney, New South Wales, Australia

Correspondence
Bin Sheng, Department of Computer Science and Engineering, Shanghai Jiao Tong University, Shanghai 200240, China.
Email: shengbin@sjtu.edu.cn

Funding information
National Natural Science Foundation of China, Grant/Award Numbers: 61872241, 61572316

Abstract

Angle closure glaucoma leads to fluid deposition in eye, and intraocular pressure occurs that damage the optic nerve, causes blindness and vision loss. Anterior chamber (AC) evaluation is imperative for determining the risk of angle-closure. Previously, techniques were dependent on either Pentacam–Scheimpflug that interprets poor visual information, anterior segment optical coherence tomography is injurious to intercede opaque optical structures. Therefore, in this paper, an experimental protocol is designed for detailed disease analysis based on IBM SPSS statistics via ultrasound biomicroscopy which is superior in evaluating deep structures; first, the affected parameter for AC is analysed, and afterwards the direction that needs laser surgery is explored. Experiments are conducted on large-scale clinical studies from an affiliated hospital in Shanghai, China. The dataset comprised 600 AC images in five directions of 60 subjects. The mean with standard deviation for anterior open distance is 0.15879±0.096779 mm, 0.15863±0.081435 mm, and anterior chamber angle is 18.749±08.0315°, 18.741±08.3889° for left and right eye respectively. It is found that anterior chamber angle in the downside of the AC is wider than the upside. However, this decision is partly based on the narrowest part of the angle to widen the depth of the direction and eliminate pupil block.

1 | INTRODUCTION

Anterior chamber (AC) dimensions are essential for the accurate assessment of medical applications. A precise measurement of anterior chamber angle (ACA) and anterior chamber depth (ACD) is necessary to diagnose angle closure glaucoma (ACG) [1]. ACG is commonly originate in Asians 87%, and generate 55 million persons consensual anopsia by 2020 [2, 3]. ACG is the second leading cause of glaucoma, but its possessions are additional critical because of a high rate of sightlessness instead of primary open-angle glaucoma [4, 5]. ACG occurs due to fluid in front part of the eye; while the capacity of fluid upsurges, the compression is building in the eye, which destruct optic nerve [6, 7]. AC visualisation and analysis is significant for ACG detection [8].

Previously, we had different techniques for the clinical assessment of AC. Gonioscopy [9] represented the standard gold method for clinical assessment of AC structures and configurations. Conversely, the Gonioscopy analysis is distinctive, extremely reliant on the doctor's ability and patient's

collaboration. Due to the rapid growth of innovative imaging procedures of the anterior segment, new imaging models, like Pentacam–Scheimpflug imaging [10], anterior segment optical coherence tomography (AS-OCT) [11, 12] have been developed and also commercially accessible. These innovative models have increased the different conventional image policies, including Orbscan scanning-slit topography (SL-OCT) and ultrasound biomicroscopy (UBM) [13]. These image modalities are used to measure quantitative and qualitative assesment of the cornea and anterior chamber. SL-OCT is an alternative and has primarily been used to view the cornea, although it may also have applications in angle estimation. OCT (optical coherence tomography) is cost-effective, provides resolution, but harmful to interceded optical opaque structures comprises of normal anatomy (sclera, iris) and pathology (haemorrhage, corneal scars, and cataract) [14]. Direct visualisation of the angle is not possible with Pentacam–Scheimpflug device, preventing the morphological assessment of the anterior chamber in cases of plateau iris or lesions of the ciliary body [15].

The angle assessment via 2D AS-OCT have poor quality [16, 17]. Limitations of both SL-OCT and AS-OCT include distortion from off-axis measurements, requiring a software correction for optical distortion and for changes in beam angulation due to the passage of light through media with different refractive qualities. Pavlin et al. were the first to quantify the anterior chamber and have suggested several parameters for objective measurement of the anterior segment [15, 18]. UBM and OCT have been proven to be the most reproducible and accurate, and therefore the most relevant to clinical decision making and patient prognosis.

UBM is superior in evaluating deep structures used for diagnostic applications and structure health monitoring of anterior ocular segment [22]. UBM is used for clinical application of the eye, in which 35 MHz frequencies or above provide a more detailed enhancement in resolution compared with regular ophthalmic ultrasound systems [14, 23]. UBM provides essential biometric information about anterior segment structures. This information helps to diagnose various deformities such as Glaucoma, cysts, cornea, and its constituent layers [24, 25]. UBM can also illustrate the rotation of the ciliary body, that stops the forward flow of aqueous which press against the lens equator during the occurrence of glaucoma [23, 26]. UBM gives the high-resolution images with a transverse resolution of 50 mm, and an axial resolution of about 25 mm [27, 28]. Unlike AS-OCT, UBM can achieve visualisation of structures posterior to the iris pigment epithelium as sound penetrates the pigment epithelium but light does not [29].

Therefore, in this paper, an analysis is performed for detailed disease assessment based on UBM. The AC analysis is comprised of different parameters in this paper showing in Figure 1. Existing techniques that include AS-OCT, 2D-CAS-OCT, 3D-AS-OCT, and UBM have measured other parameters analysis in different directions shown in Figure 2. Previously, AS-OCT has measured AOD_{500} and performed research in the nasal and temporal direction, 2D-CAS-OCT and 3D-AS-OCT have measured ACD, UBM has measured ACD, ACA, AOD_{500} and only AOD_{500} performed an analysis in inferior, nasal, temporal directions. Therefore, in this paper, we have performed analysis to evaluate all the parameters in five different directions to get the affected parameter information and direction for surgery.

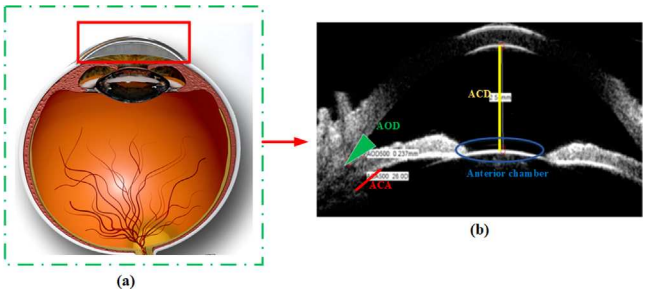

FIGURE 1 (a) The anterior segment region of the eye contains the cornea, iris, lens, and ciliary body with UBM. (b) Anterior chamber contains ACA, AOD, and ACD. AOD is the distance from the cornea to iris at 500 μm from the scleral spur, ACD is the anterior chamber depth that is measured along the perpendicular line

We have no reliable method yet for the parameter evaluation, so we are trying to design an experimental protocol. Therefore, in this study, we would focus on developing an experimental protocol for analysing AC. The experimental protocol is intended to provide details about the affected AC parameter and its direction for laser surgery.

1.1 | Parameters of AC

To summarise, this work has the three following contributions:

- **Detailed disease analysis**: An experimental protocol is designed for angle-closure glaucoma based on UBM. This protocol is used to measure the parameters of the anterior chamber. Parameters include anterior chamber depth (ACD), anterior chamber angle (ACA), and anterior open distance (AOD).
- **Planning surgery**: The analysis helps doctors to validate the affected parameter and also provide direction information for laser surgery. Each parameter is measured in five different directions, i.e. nasal, temporal, down, up (with-ACD), and up (without-ACD).
- **Dataset formulation**: A large-scale dataset is designed, and experimental valuation is performed with Shanghai Sixth People Hospital. Currently, there are no such datasets available. The designed dataset contains three parameters in five different directions.

The rest of the paper is organised as follows. Section 2 introduces the related work on image modalities. Section 3 describes experimental protocol. Experimental analysis and results are discussed in Section 4. Finally, section 5 concludes research and provides some future directions.

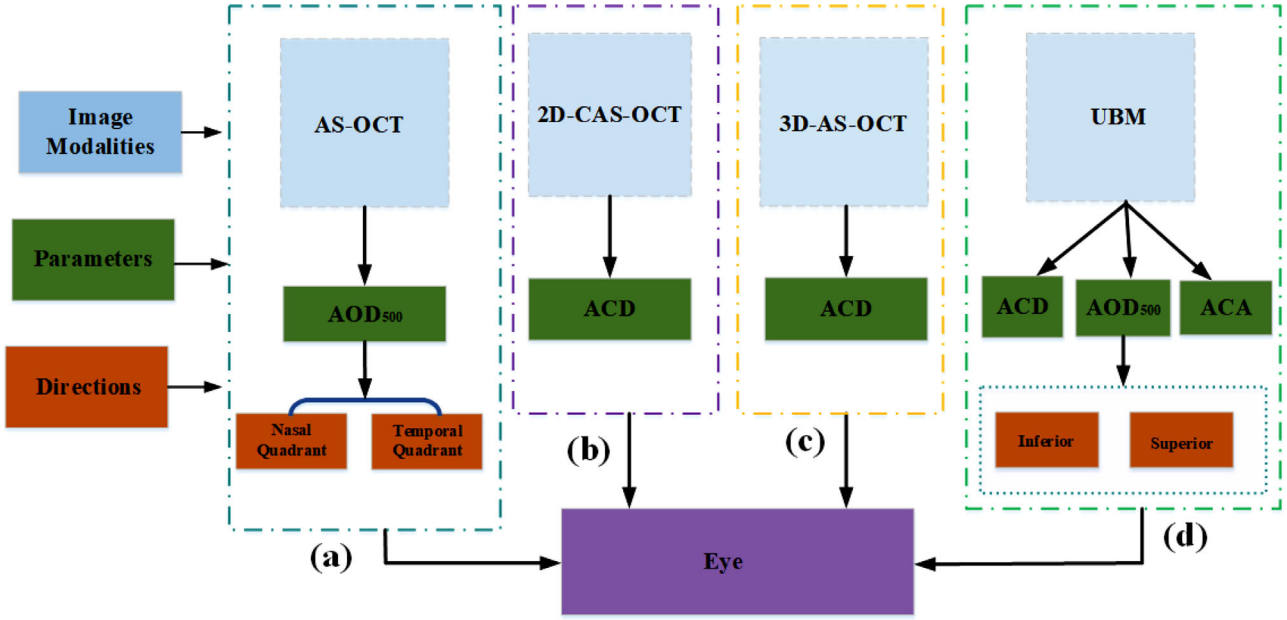

FIGURE 2 Architecture of existing image modalities with different parameters analysis. (a) AS-OCT has measured parameter AOD_{500} in two directions contain nasal quadrant and temporal quadrant [19] . (b) 2D-CAS-OCT measured parameter ACD [20]. (c) 3D-AS-OCT has measured ACD [20]. (d) UBM has measured AOD_{500} in two directions, i.e. superior and inferior [21]

2 | RELATED WORK

Each method has its specific benefits and drawbacks relative to each other. Gonioscopy grading systems are used to record finding using a systematic approach, and still represents a method for detailed visualisation of the iridocorneal angle architecture. Gonioscopy is time-consuming and uncomfortable for the patient but sometimes it is difficult to use in cases of damaged corneal epithelium or infections disorder [10]. The same limitations can be taken while exploring the anterior segment using OCT, it renders simple qualitative information that is capable of guiding through the clinical assessment with thin or closed angles, mainly when gonioscopy is hard to apply or understand [10]. Anterior segment OCT may be helpful in clinical situations for glaucoma patients but angle assessment is shown to have poor quality compared with UBM [30, 31]. Ultrasound (US) imaging gives a consistent result and accomplished in obtaining transmural material through tissue wall [32]. Optically based systems that mentioned above, are incomplete through the existence of optical opacities of ordinary anatomy [14]. Existing techniques have measured some of the parameters showing in Figure 2. Existing clinical ultrasound systems are intelligent enough to generate real-time high-resolution images with a rate of more than 7,000 frames/second [8]. The frame rate of US imaging systems is high like 10,000 frames/second [8], and the corresponding result is accomplished for attaining transmural data by tissues wall. US is used for the surgery of deep structures [32, 33]. In this paper, we are focusing on UBM. UBM gives high resolution to the images with a depth of 5 mm [13, 27] in tissues. UBM system emphasises on the processing of raw information attained and appropriate in progressive planes for 3D analysis, specifically for corneal biometric analysis.

3 | EXPERIMENTAL PROTOCOL

In this section, an experimental protocol is designed for Glaucoma detection and for planning laser surgery based on UBM as shown in Figure 3. Dataset formulation, biometric measurements, and established protocol are included in the experimental protocol.

3.1 | Dataset formulation

In this section, the dataset is formulated for measurements of parameters. A formulated dataset of the AC includes three parameters for right and left eyes in five directions. Directions include down, nasal, temporal, up (with-ACD), and up (without-ACD). The median age of all subjects was (20–54) years. The dataset comprises 600 AC images in five directions of 60 patients by 10 samples per patient (five each). Subjects were successively engaged for clinical inspection. In addition, patients were trained to look at UBM with an internal fixation target during scanning. According to our best acquaintance, no online dataset is available for the AC parameters analysis measured with UBM. US imaging has been revolutionised in the last few years due to the accessibility of transducers that are used for the working of wide range frequencies, because of the suitability of fast speed, and high-resolution [25, 34, 35].

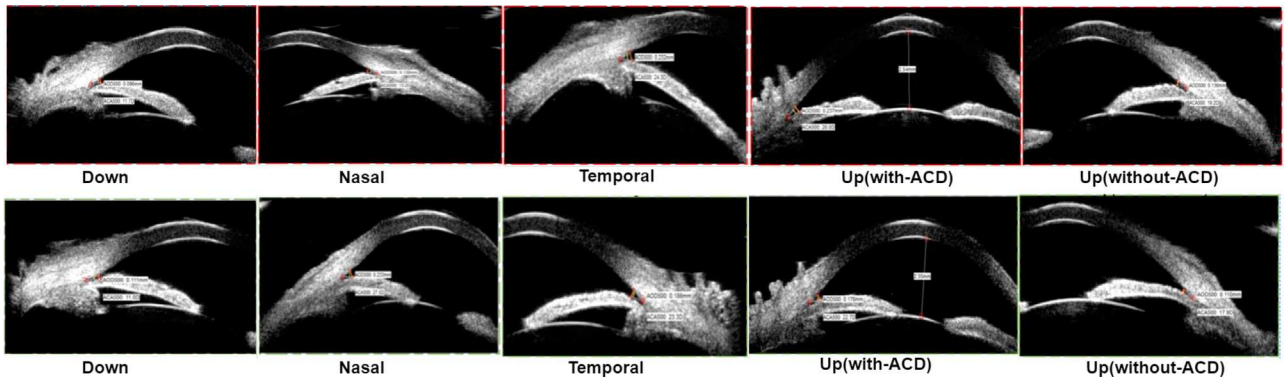

FIGURE 3 The experimental protocol is designed for the measurements and direction analysis by UBM. The experimental protocol provides us detailed disease analysis about the affected parameter and helps to give directions for planning laser surgery. (a) Right eye in five different angle directions: down, nasal, temporal, up (with-ACD), and up (without-ACD). (b) Left eye in five different angles, i.e. down, nasal, temporal, up (with-ACD), and up (without-ACD)

3.2 | Biometric measurements

All the measurements are recorded between 10:00 PM to 5:00 PM in the absence of pupil dilation. The inspection room is illumined 6.0 ± 1.5 lux, and that illumination is measured by a light meter (LM-8000, Fuso). In the same illuminated environments, two ophthalmologists have collected the measurements with UBM. This study has been done by UBM (UD-6000, TOMEY Co. Ltd, Japan) device and a sample of SUOWEI device, at Shanghai Sixth People's Hospital, China. The sample is similar for scanning-source ultrasound technology, with high sensitivity less than 0.05mm and rapid measurement speed 50 MHz [18, 36–38]. Device is attached to an arm that allows careful placement over the patient eye. Scanning-source ultrasound used high-speed wavelength, and spectrometer. This device has measured the maximum width and depth 16 mm×9 mm, 5.5 mm of tissues respectively with a speed of 20,000 A-lines/s [31, 39]. The mean axial resolution is 2.2 mm with 20 μm deep tissue. The cross resolution of the attained image is <50 μm [40–42]. The acquisition time is 5 s/volume with resolution of 256 voxels ×256 voxels×1024 voxels, the time of 256 A-scans per 1 cross-section image is 5 to 10 s [38], [43]. A typical 3D scans are split into 256 horizontal cross-sections, contains 256 A-scans individually.

3.3 | Established protocol

This study was approved by the ethics committee of Sixth People's Hospital Affiliated of Shanghai Jiaotong University, Shanghai, China. Sixty-five Chinese patients (650 eyes) were enrolled from the Department of Ophthalmology. Written, informed consent was obtained from all patients. The patients were randomly divided into two groups using a random number table. The inclusion criteria were patients with a relatively narrow AC suspected to do laser peripheral iridotomy operation. The patients with a history of break out of acute ACG, or ocular disease that may cause secondary angle closure, such as AC inflammation, previous ocular surgery, or systemic diseases, such as diabetes mellitus, were excluded from our study. Previously, existing techniques [26, 44] have measured parameters in different directions with different conditions like AS-OCT has measured AOD_{500} in two directions, i.e. nasal quadrant and temporal quadrant [19]. 2D-CAS-OCT and 3D-AS-OCT have measured ACD [20, 45]. UBM has measured AOD_{500} in two direction, i.e. superior and inferior [46]. The designed protocol for this paper analyses Glaucoma affected parameter and also helps to validate the specific direction that needs laser surgery. For this, statistical analysis is performed using the IBM SPSS Statistics 22.lnk. A pipeline is designed for the detection of AC shown in Figure 4.

Experimental protocol worked on two steps. The first is to analyse the parameters for Glaucoma, and the second is to analyse the direction for surgery. For the first step, the parameters are analysed by compare means. In SPSS Statistics, compare means are of five types, i.e. means, one-sample *t*-test, independent samples test, paired-samples *t*-test, and one-way-ANOVA. To analyse parameters for Glaucoma detection, we have compared means. To compare the mean, a dependent and independent list is required. Parameters names are included in the independent list, and the parameters values are included independent list. Second is the analysis of direction for planning surgery is performed by non-parametric tests. In non-parametric tests, conditions are not explained by the models about the parameters, and no need for strong measurements. Non-parametric tests can be applied on an ordinal scale and in a nominal scale dataset. Non-parametric tests can be applied on three types, first is one-sample test that analyses one field, second is a test for related samples that compare two or more fields for the same set of the case, a third is an independent-samples test analyses one field that is grouped by categories of another area.

An independent sample for non-parametric tests has been selected that can easily differentiate the differences between two or more groups. independent samples can analyse by automatically compare distributions across groups. After this, customise tests option has been selected, i.e. the first is Mann–Whitney U for two groups, and the second is Kruskal–Wallis

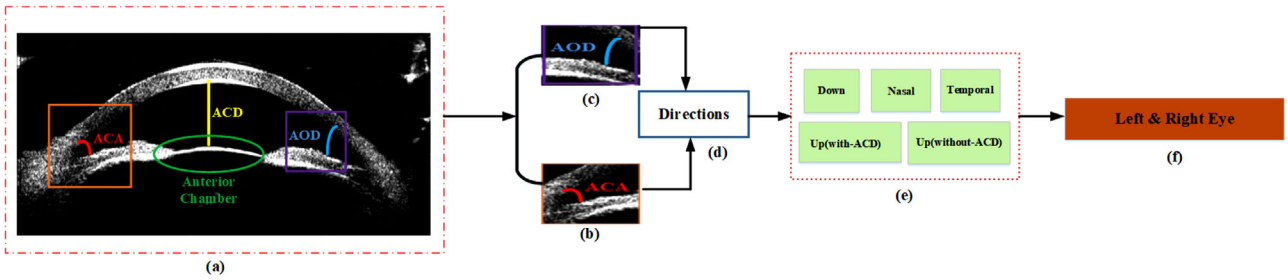

FIGURE 4 Pipeline designed for ACG detection. (a) AC visualisation helps to diagnose ACG. ACD was measured along the perpendicular line at a 90-degree (yellow line), ACA on the left side in an orange box. And the AOD measured from the cornea to the iris at 500 μm from the scleral spur. (b, c) After the evaluation analysis of affected parameters, analysed direction for laser surgery. AOD and ACA include five directions given in (e). (f) These three parameters are measured for the left and right eyes

1-way ANOVA for more than two groups. We have chosen Kruskal–Wallis 1-way ANOVA. Statistical analysis was performed with a non-parametric test. An independent sample for non-parametric tests has been selected that can easily differentiate the differences between two or more groups. After this, we have performed customised tests, including Kruskal–Wallis 1-way ANOVA for more than two groups for pairwise comparison. The criteria for significance difference is 0.05. So in refs. [1–4] there is statistical difference in up–temporal directions.

P values of less than 0.05 were considered statistically significant for all statistical analysis. This has been concluded from the statistical difference that the width of the temporal side is the widest, and the upside is the narrowest direction. So, most of the doctors select the upside for laser surgery. The decision is usually not based on the narrowest part of the angle. Some doctors chose the superior aspect of the chamber angle.

4 | EXPERIMENTAL RESULTS

Innovative work is presented for the AC using UBM and is shown in Figure 4. Experiment protocol is showing in Figure 3.

4.1 | Measurement of parameters for left and right eye

The subjects experienced a full ophthalmic examination comprised of the measurement of AOD, ACA, and ACD. UBM has high speed, and best in evaluation of deep structures; therefore, ACD, ACA, and AOD can be easily measured. UBM is used to measure and visualise the parameters and involves direct contact among probe and eye. Detailed disease analysis is performed using SPSS statistics based on anterior chamber parameters. First, we analyse the glaucoma affected parameter by comparing Means. By comparing Means, we analyse that the ACA value for left and right is high compared to AOD (left and right eye). Afterwards, another analysis about laser direction is performed. For this a pairwise comparison of direction has been performed by comparing each direction with others in a pair. The values for pairwise directions comparison shown in Tables 1–4. The value in up (with-ACD)–temporal direction is high in ACA and AOD for left and right eye.

Tables 1–4 show the non-parametric pairwise comparison between each directions. The marked red and yellow coloured box showed in the table, as mentioned earlier, shows that there is a significant difference in the pairwise directions. Table 1, is pairwise comparison of right eye AOD which shows significant

TABLE 1 Pairwise directions of right eye AOD (mm)

Directions (1–2)	Test statistics	Adj. significant
Up (with-ACD)–up (without-ACD)	−4.266	1.000
Up (with-ACD)–nasal	15.688	1.000
Up (with-ACD)–down	29.922	0.252
Up (with-ACD)–temporal	42.328	0.003
Up (without-ACD)–nasal	11.422	1.000
Up (without-ACD)–down	21.656	0.615
Up (without-ACD)–temporal	38.062	0.010
Nasal–down	10.234	1.000
Nasal–temporal	−26.641	0.214
Down–temporal	−16.406	1.000

TABLE 2 Pairwise directions of left eye AOD (mm)

Directions (1–2)	Test statistics	Adj. significant
Up (without-ACD)–up (with-ACD)	0.226	1.000
Up (without-ACD)–down	20.258	0.754
Up (without-ACD)–nasal	24.113	0.343
Up (without-ACD)–temporal	40.000	0.004
Up (with-ACD)–down	20.032	0.788
Up (with-ACD)–nasal	23.887	0.361
Up (with-ACD)–temporal	39.774	0.005
Down–nasal	−3.855	1.000
Down–temporal	−19.742	0.832
Nasal–temporal	−15.887	1.000

TABLE 3 Pairwise directions comparison of right eye ACA (D)

Directions (1-2)	Test statistics	Adj. significant
Up (with-ACD)–up(without-ACD)	−10.094	1.000
Up (with-ACD)–nasal	13.531	1.000
Up (with-ACD)–down	28.109	0.152
Up (with-ACD)–temporal	45.297	0.001
Up (without-ACD)–nasal	03.438	1.000
Up (without-ACD)–down	18.016	1.000
Up (without-ACD)–temporal	35.203	0.024
Nasal–down	14.578	1.000
Nasal–temporal	−31.766	0.061
Down–temporal	−17.188	1.000

TABLE 4 Pairwise directions comparison of left eye ACA (D)

Directions (1-2)	Test statistics	Adj. significant
Up (without-ACD)–up (with-ACD)	0.581	1.000
Up (without-ACD)–nasal	16.581	1.000
Up (without-ACD)–down	16.871	1.000
Up (without-ACD)–temporal	36.048	0.016
Up (with-ACD)–nasal	16.000	1.000
Up (with-ACD)–down	16.290	1.000
Up (with-ACD)–temporal	35.468	0.019
Nasal–down	0.290	1.000
Nasal–temporal	−19.468	0.877
Down–temporal	−19.177	0.926

TABLE 5 Anterior chamber parameters measured with UBM

Parameters	Directions	Mean	Std. deviation
Left eye ACA (D)	Down	19.129	09.0999
	Nasal	19.700	08.8819
	Temporal	21.919	07.6163
	Up (with-ACD)	16.594	07.0029
	Up (without-ACD)	16.403	06.3581
	Total	18.749	08.0315
Left eye AOD (mm)	Down	0.15929	0.089206
	Nasal	0.19006	0.153039
	Temporal	0.18523	0.077493
	Up (with-ACD)	0.12900	0.059772
	Up (without-ACD)	0.13039	0.060307
	Total	0.15879	0.096779
Right eye AOD (mm)	Down	0.16475	0.070953
	Nasal	0.15094	0.067805
	Temporal	0.20166	0.091813
	Up (with-ACD)	0.14325	0.101336
	Up (without-ACD)	0.13253	0.052204
	Total	0.15863	0.081435
Right eye ACA (D)	Down	19.850	08.00921
	Nasal	17.388	07.0564
	Temporal	24.078	10.01113
	Up (with-ACD)	15.697	07.06820
	Up (without-ACD)	16.694	06.01614
	Total	18.741	08.03889

difference in (up (with-ACD)–temporal)=0.003 and (up(without-ACD)–temporal = 0.010. In Table 2, the pairwise comparison for AOD for left eye shows that there is significant difference in the pair of two directions, i.e. (up (without-ACD)–temporal)= 0.004, and (up (with-ACD)–temporal)=0.005. Table 3, shows comparison of right eye ACA with significant difference in two pair of direction, i.e. (up (with-ACD)–temporal)=0.001 and the other is (up (without-ACD)–temporal)=0.024. The pairwise comparison of left eye ACA

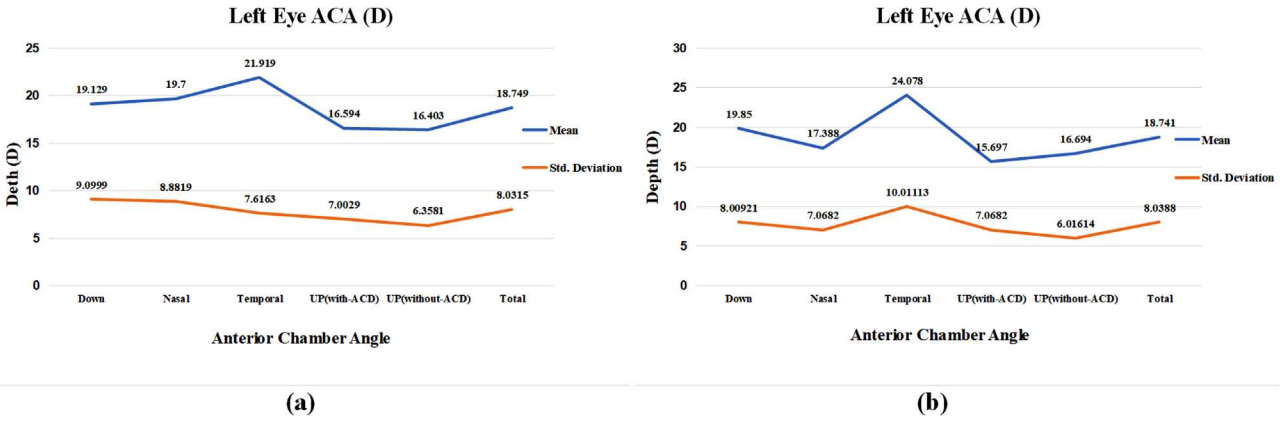

FIGURE 5 AC analysis includes Mean and Std. dev. On the *x*-axis, ACA is given, and on the *y*-axis number of ACD is given. (a) Analysis of left eye. (b) Analysis of right eye. In (a) and (b), it is clearly showing that the mean in temporal directions is high, which helps doctors to perform laser surgery. Mean in temporal directions are most comprehensive, and the upside is the narrowest side

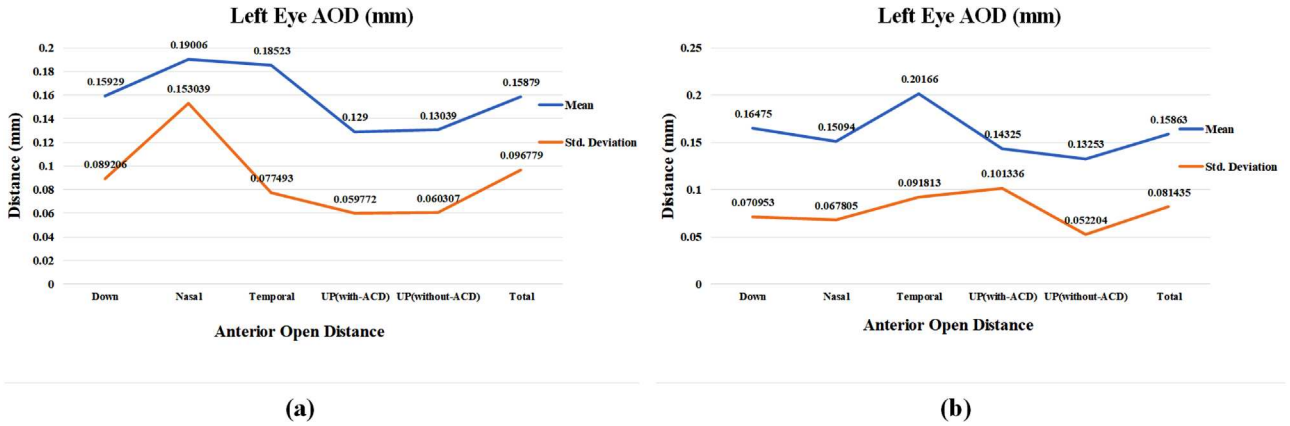

FIGURE 6 AOD analysis that includes Mean and Std. dev. (a) Analysis of left eye. (b) Analysis of right eye. There is a vast difference in temporal directions, clearly shown in the mean and std. dev. of ACA and AOD

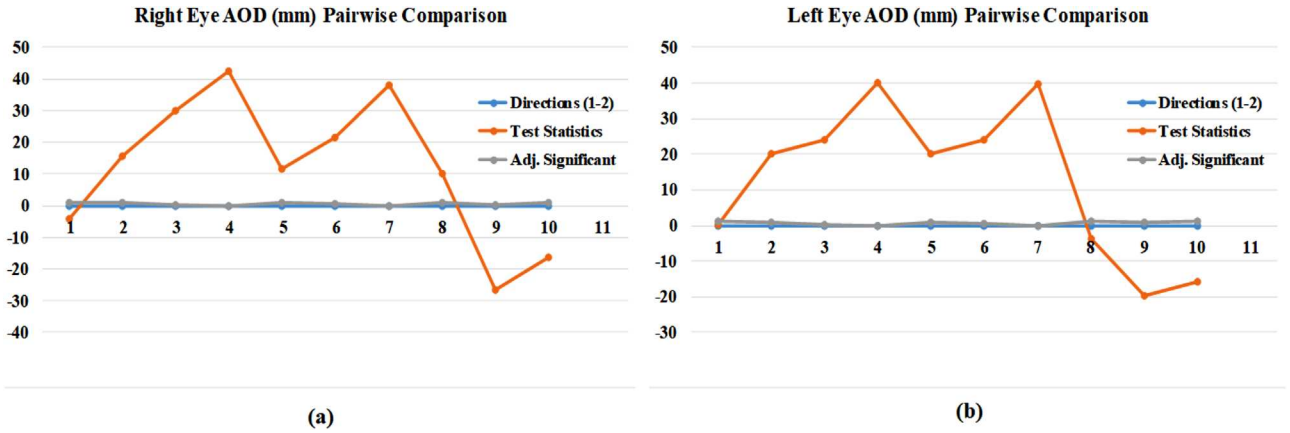

FIGURE 7 Statistical difference of AOD. (a) Pairwise comparison of the left eye. (b) Pairwise comparison of the right eye. There is a difference between the width. The ACA in the downside of the anterior chamber is wider than the upside. Temporal directions are the widest side, and the upside is the narrowest

is shown in Table 4 with a significant difference in two pairs of directions that are (up (without-ACD)–temporal)=0.016, and (up (with-ACD)–temporal)=0.019. This is the study that measures the parameters of the anterior chamber using UBM; measuring AC dimensions are significant for planning surgery. Table 5 shows the mean with standard deviation for AOD are 0.15879 ± 0.096779 mm, 0.15863 ± 0.081435 mm and ACA is $18.749 \pm 08.0315°$, $18.741 \pm 08.3889°$ for left and right eye respectively.

4.2 | Why up(ACD) has high value in ACA and AOD?

The graph for these parameters is shown in Figures 5 and Figure 6. In Figures 7, and 8 it is found that there is a significant difference between the width of ACA and AOD from different directions. The ACA in the downside of the anterior chamber is wider than the upside. The width of the temporal side is the widest, and the upside is the narrowest direction. Some doctors chose the superior part of the chamber angle because the hole created by Nd:YAG laser is covered by the superior eyelid, which avoids possible photic phenomena (in most cases). So, the decision is partly based on the narrowest part of the angle to widen the depth of this direction and eliminate pupil block. UBM produced eight-frames of cross-sectional images per second, and for capturing, the image uses sound waves through opaque media. OCT uses light waves that cannot penetrate the tissues.

5 | CONCLUSION

This paper presents an experimental protocol for AC parameters in five different directions for ACG detection. An AC detection provides detailed disease analysis. This analysis not only provided information about the particular disease-affected area of the AC but also provided information about the direction that needs laser surgery. Experimental protocol concludes that there is a significant difference between ACA (D) and AOD (mm) from different directions. The ACA's downside is more comprehensive than the upside due to the force of gravity. In the temporal direction, the width is wide, and the upside is narrowest. The decision is limited to the upside, but some doctors

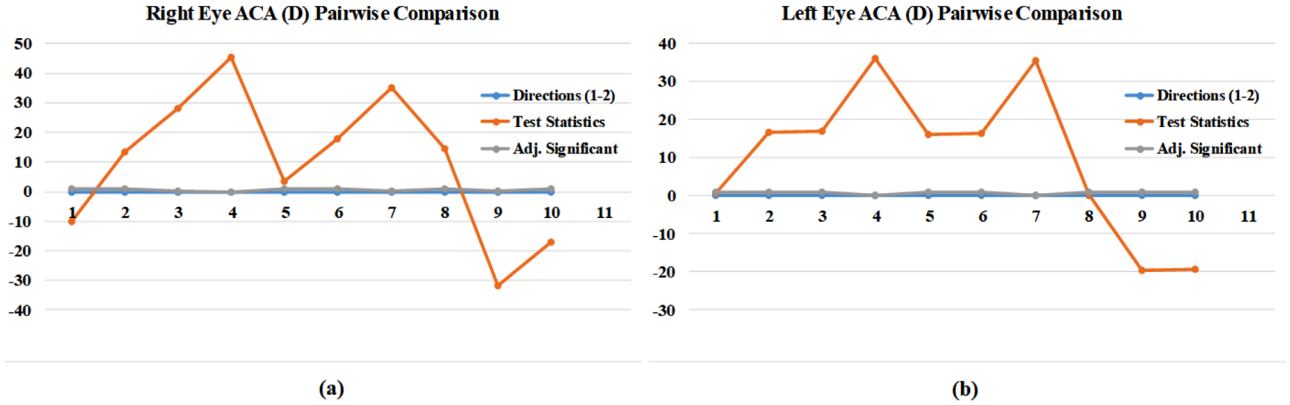

FIGURE 8 Statistical difference of ACA. (a) Pairwise comparison of the left eye. (b) Pairwise comparison of the right eye. A pairwise comparison shows the comparison between two directions. And by comparison, we have concluded that there is a difference in the width of ACA in different directions

also chose the only partly because the hole created by ND:YAG laser is also covered by the inferior eyelid, which avoids possible photic phenomena (in most cases). So the decision is partially based on the narrowest part of the angle to widen the depth of this direction and eliminate pupil block. A large-scale dataset is designed for parameter analysis of the AC. In the future, we will increase the dataset of normal patients. Currently, this protocol works for parameters, i.e. AOD, ACA, and ACD, with five different directions. We will extend it by adding other parameters of the AC.

ACKNOWLEDGMENTS

This work was supported in part by the National Natural Science Foundation of China under Grant 61872241 and 61572316.

CONFLICT OF INTEREST

The authors declare no conflict of interest.

DATA AVAILABILITY STATEMENT

There is no publicly dataset available for this research manuscript.

ORCID

Saba Ghazanfar Ali https://orcid.org/0000-0003-2682-8300
Riaz Ali https://orcid.org/0000-0002-0404-1227
Bin Sheng https://orcid.org/0000-0001-8678-2784
Ping Li https://orcid.org/0000-0002-1503-0240

REFERENCES

1. Yassa, E.T., Ünlü, C.: Anterior chamber angle and volume do not change after myopic laser-assisted in situ keratomileusis in young patients. J. Ophthalmol. 2018, 8646275 (2018)
2. Tian, J., Marziliano, P., Baskaran, M., Wong, H.T., Aung, T.: Automatic anterior chamber angle assessment for HD-OCT images. IEEE Trans. Biomed. Eng. 58(11), 3242–3249 (2011)
3. Fu, H., Xu, Y., Lin, S., Zhang, X., Wong, D.W.K., Liu, J., et al.: Segmentation and quantification for angle-closure glaucoma assessment in anterior segment OCT. IEEE Trans. Med. Imaging 36(9), 1930–1938 (2017)
4. Li, M., Chen, Y., Chen, X., Zhu, W., Chen, X., Wang, X., et al.: Differences between fellow eyes of acute and chronic primary angle closure (glaucoma): an ultrasound biomicroscopy quantitative study. PloS One 13(2), e0193006 (2018)
5. Ram, S., Danford, F., Howerton, S., Rodríguez, J.J., Geest, J.P.V.: Three-dimensional segmentation of the ex-vivo anterior lamina cribrosa from second-harmonic imaging microscopy. IEEE Trans. Biomed. Eng. 65(7), 1617–1629 (2017)
6. Maheshwari, S., Pachori, R.B., Acharya, U.R.: Automated diagnosis of glaucoma using empirical wavelet transform and correntropy features extracted from fundus images. IEEE J. Biomed. Health. Inf. 21(3), 803–813 (2017)
7. Do, T., Xuan, H.N., Lam, H.D., Tien, D.T., Thuy, G.N.T., Ngoc, H.N.D., et al.: Ultrasound biomicroscopic diagnosis of angle-closure mechanisms in vietnamese subjects with unilateral angle-closure glaucoma. J. Glaucoma 27(2), 115–120 (2018)
8. Kondapalli, S.H., Alazzawi, Y., Malinowski, M., Timek, T., Chakrabartty, S.: Multiaccess in vivo biotelemetry using sonomicrometry and M-scan ultrasound imaging. IEEE Trans. Biomed. Eng. 65(1), 149–158 (2017)
9. Barkana, Y., Dorairaj, S.K., Gerber, Y., Liebmann, J.M., Ritch, R.: Agreement between gonioscopy and ultrasound biomicroscopy in detecting iridotrabecular apposition. Arch. Ophthalmol. 125(10), 1331–1335 (2007)
10. Raluca, M., Mircea, F., Andrei, F., Carmen, D., Miruna, N., Grigorios, T., et al.: Old and new in exploring the anterior chamber angle. Rom. J. Ophthalmol. 59(4), 208–216 (2015)
11. Mak, H., Xu, G., Leung, C.K.S.: Imaging the iris with swept-source optical coherence tomography: relationship between iris volume and primary angle closure. Ophthalmology 120(12), 2517–2524 (2013)
12. Leung, C.K.s., Yung, W.h., Yiu, C.K.f., Lam, S.w., Leung, D.Y.l., Tse, R.K.k., et al.: Novel approach for anterior chamber angle analysis: anterior chamber angle detection with edge measurement and identification algorithm (academia). Arch. Ophthal. 124(10), 1395–1401 (2006)
13. Chen, Q., Ma, R., Gan, L., Ren, H., Yuan, Y.: Value of ultrasound biomicroscopy in assessment of small masses at medial canthal region. Graefe's Arch. Clin. Exp. Ophthalmol. 257(4), 827–834 (2019)
14. Silverman, R.H.: High-resolution ultrasound imaging of the eye–a review. Clin. Exp. Ophthalmol. 37(1), 54–67 (2009)
15. Ali, S.G., Chen, Y., Sheng, B., Li, H., Wu, Q., Yang, P., et al.: Cost-effective broad learning-based ultrasound biomicroscopy with 3d reconstruction for ocular anterior segmentation. Multimedia Tools Appl. 80, 35105–35122 (2020)
16. Lata, S., Venkatesh, P., Temkar, S., Selvan, H., Gupta, V., Dada, T., et al.: Comparative evaluation of anterior segment optical coherence tomography, ultrasound biomicroscopy, and intraocular pressure changes after panretinal photocoagulation by pascal and conventional laser. Retina 40(3), 537–545 (2018)
17. Fu, H., Cheng, J., Xu, Y., Zhang, C., Wong, D.W.K., Liu, J., et al.: Disc-aware ensemble network for glaucoma screening from fundus image. IEEE Trans. Med. Imaging 37(11), 2493–2501 (2018)

18. Yan, X., Tang, G., Zhang, H., Li, F.: Ultrasound biomicroscopy characteristics of late capsular block syndrome before and after treatment. JCRS Online Case Rep. 7(1), 9–10 (2019)
19. Narayanaswamy, A., Sakata, L.M., He, M.G., Friedman, D.S., Chan, Y.H., Lavanya, R., et al.: Diagnostic performance of anterior chamber angle measurements for detecting eyes with narrow angles: an anterior segment OCT study. Arch. Ophthalmology 128(10), 1321–1327 (2010)
20. Fukuda, S., Kawana, K., Yasuno, Y., Oshika, T.: Repeatability and reproducibility of anterior ocular biometric measurements with 2-dimensional and 3-dimensional optical coherence tomography. J. Cataract Refractive Surg. 36(11), 1867–1873 (2010)
21. Friedman, D.S., He, M.: Anterior chamber angle assessment techniques. Surv. Ophthalmol. 53(3), 250–273 (2008)
22. Guo, X., Wu, N., Zhou, J., Du, C., Wang, X.: Ultrasound generation from side wall of optical fibers. In: 2017 16th International Conference on Optical Communications and Networks (ICOCN), pp. 1–3. IEEE, Piscataway, NJ (2017)
23. Shahid, H., Salmon, J.: Malignant glaucoma: a review of the modern literature. J. Ophthalmol. 2012, 852659 (2012)
24. Huang, Q., Lan, J., Li, X.: Robotic arm based automatic ultrasound scanning for three-dimensional imaging. IEEE Trans. Ind. Inf. 15(2), 1173–1182 (2019)
25. Chen, Q., Gu, J., Jiang, R., Zhou, M., Chang, Q.: Role of ultrasound biomicroscopy in diagnosis of ocular toxocariasis. Br. J. Ophthalmol. 102(5), 642–646 (2018)
26. Sadaka, A., Prager, T., Beaver, H., Malik, A.: A novel use of ultrasound biomicroscopy. Eye 32(2), 474 (2018)
27. Konstantopoulos, A., Hossain, P., Anderson, D.F.: Recent advances in ophthalmic anterior segment imaging: a new era for ophthalmic diagnosis? Br. J. Ophthalmol. 91(4), 551–557 (2007)
28. Choi, K.H., Choo, S.W., Jeong, S.W., Kim, J.Y.: Ultrasound biomicroscopy studies to evaluate ciliary cleft parameters in healthy eyes of American cocker spaniels. Pak. Vet. J. 39(1), 66–70 (2019)
29. Rojas, J.D., Papadopoulou, V., Czernuszewicz, T.J., Rajamahendiran, R.M., Chytil, A., Chiang, Y.C., et al.: Ultrasound measurement of vascular density to evaluate response to anti-angiogenic therapy in renal cell carcinoma. IEEE Trans. Biomed. Eng. 66(3), 873–880 (2018)
30. Lim, S.H.: Clinical applications of anterior segment optical coherence tomography. J. Ophthalmol. 2015, 605729 (2015)
31. Kaushik, S., Pandav, S.: Ultrasound biomicroscopy in glaucoma. In: Hema, H.V., Hema, N. (eds.) Gems of Ophthalmology: Glaucoma, p. 61. Jaypee Brothers Medical Publishers, New Delhi (2018)
32. Wang, X., Seetohul, V., Chen, R., Zhang, Z., Qian, M., Shi, Z., et al.: Development of a mechanical scanning device with high-frequency ultrasound transducer for ultrasonic capsule endoscopy. IEEE Trans. Med. Imaging 36(9), 1922–1929 (2017)
33. Chen, S.T., Guo, L.H., Yan, J.N., Wang, Q., Li, X.L., Li, M.X., et al.: Ultrasound biomicroscopy and high-frequency ultrasound for evaluating extramammary paget disease with pathologic correlation. J. Ultrasound Med. 38(12), 3229–3237 (2019)
34. Shi, Y., Wang, H., Han, Y., Cao, K., Vu, V., Hu, M., et al.: Correlation between trabeculodysgenesis assessed by ultrasound biomicroscopy and surgical outcomes in primary congenital glaucoma. Am. J. Ophthalmol. 196, 57–64 (2018)
35. Saba, T., Bokhari, S.T.F., Sharif, M., Yasmin, M., Raza, M.: Fundus image classification methods for the detection of glaucoma: a review. Microsc. Res. Tech. 81(10), 1105–1121 (2018)
36. Wu, N., Zhang, H., Chen, B., Ding, W.: A novel application of b-ultrasonography at various head positions in the diagnosis of untypical uveitis-glaucoma-hyphema (UGH) syndrome: a case report. Medicine 98(2), e13891 (2019)
37. Jindal, A., Ctori, I., Virgili, G., Lucenteforte, E., Lawrenson, J.G.: Non-contact methods for the detection of people at risk of primary angle closure glaucoma. Cochrane Database Syst. Rev. 2018(2), CD012947 (2018)
38. Martin, R.: Cornea and anterior eye assessment with slit lamp biomicroscopy, specular microscopy, confocal microscopy, and ultrasound biomicroscopy. Ind. J. Ophthalmol. 66(2), 195 (2018)
39. Masna Hidalgo, B.J., Lopez, V.B., Concepcion, M.E.T., Sibayan, S.A.: Ciliary sulcus diameter measurements in normal adult Filipino eyes using ultrasound biomicroscopy. Philipp. J. Ophthalmol. 42(1), (2018)
40. Shi, M.Y., Han, X., Zhang, J.S., Yan, Q.C.: Comparison of 25 MHz and 50 MHz ultrasound biomicroscopy for imaging of the lens and its related diseases. Int. J. Ophthalmol. 11(7), 1152 (2018)
41. Hunter, N., Sayed, K., Abdel Hay, R., Allam, R., Hussein, N.: Comparing the efficacy of mesotherapy to topical minoxidil in the treatment of female pattern hair loss using ultrasound biomicroscopy: A randomized controlled trial. Acta Dermatovenerol. Croat. 27(1), 1–1 (2019)
42. Liu, Q., Dong, Y., Haijun, L., Wang, Y., Huang, Y., Dong, L., et al.: Association of anterior chamber angle open parameters with postoperative intraocular pressure following laser peripheral iridotomy. Chin. J. Exp. Ophthalmol. 36(4), 289–293 (2018)
43. Gao, K., Li, F., Li, Y., Li, X., Huang, W., Chen, S., et al.: Anterior choroidal thickness increased in primary open-angle glaucoma and primary angle-closure disease eyes evidenced by ultrasound biomicroscopy and SS-OCT. Invest. Ophthalmol. Visual Sci. 59(3), 1270–1277 (2018)
44. Helal, J., Saad, H., Sabry, M., Eldorghamy, A., et al.: Assessment of the changes in anterior segment parameters by ultrasound biomicroscopy after laser peripheral iridotomy. Delta J. Ophthalmol. 20(1), 32 (2019)
45. Wu, H., Minhaz, A.T., Helms, R., Sevgi, D.D., Yu, T., Orge, F., et al.: 3D ultrasound biomicroscopy (3D-UBM) imaging and automated 3D assessment of the iridocorneal angle for glaucoma patients. In: Medical Imaging 2019: Ultrasonic Imaging and Tomography, vol. 10955, p. 109550U. SPIE, Bellingham, WA (2019)
46. Mansouri, K., Sommerhalder, J., Shaarawy, T.: Prospective comparison of ultrasound biomicroscopy and anterior segment optical coherence tomography for evaluation of anterior chamber dimensions in European eyes with primary angle closure. Eye 24, 233–239 (2010)

How to cite this article: Ali, S., Ali, R., Sheng, B., Chen, Y., Li, H., Yang, P., Li, P., Jung, Y., Zhu, F., Lu, P., Kim, J.: Experimental protocol designed to employ Nd:YAG laser surgery for anterior chamber glaucoma detection via UBM. IET Image Process. 1–9 (2022). https://doi.org/10.1049/ipr2.12481